

ETH Hönggerberg, Zürich  
Institute of Geodesy and Photogrammetry



**GEODETTIC SEMINAR REPORT**

**GPS and INS Integration with Kalman Filtering  
for  
Direct Georeferencing of Airborne Imagery**

*Prepared by:*

**Sultan Kocaman**

*Presented to:*

**Prof. Dr. Hilmar Ingensand**

**30.01.2003**

## **CONTENTS**

### **1 Introduction**

### **2 Fundamentals of the GPS**

#### **2.1 Clocks and Time**

#### **2.2 GPS Signals**

#### **2.3 GPS Receiver**

#### **2.4 GPS Observables and Errors**

### **3 Fundamentals of Inertial Navigation**

#### **3.1 Basic Concepts of Inertial Navigation**

#### **3.2 Common Sensor Error Models**

#### **3.3 Initialization and Alignment**

#### **3.4 System-Level Error Models**

### **4 Kalman Filtering Basics**

#### **4.1 Discrete Kalman Filter**

#### **4.2 The Extended Kalman Filter**

### **5 GPS and INS Integration**

#### **5.1 Integration Modes**

#### **5.2 Integration Limitations**

### **6 A Special Application Area: Direct Georeferencing of Airborne Imagery**

### **7 Conclusions and Future Work**

## **REFERENCES**

## **APPENDIX**

### **Random Processes: Basic Concepts**

## 1 INTRODUCTION

*Georeferencing* can be defined as a process of obtaining knowledge about the origin of some event in space-time. Depending on the sensor type, this origin needs to be defined by a number of parameters such as time, position (location), attitude (orientation) and possibly also the velocity of the object of the interest. When this information is attained directly by means of measurements from sensors on-board the vehicle the term *direct georeferencing* is used [Skaloud, 1999].

For georeferencing the image data, the position ( $X_0, Y_0, Z_0$ ) and orientation ( $\omega, \varphi, \kappa$ ) of the sensor, which also are called as exterior orientation elements, should be known. Then, the uncorrected image vector is transformed to the corrected georeferenced position and the relation between the local image coordinate system and the global object frame is solved. The traditional way of georeferencing of airborne imagery is to use ground control points (GCPs) which counts a major cost for photogrammetry projects. A number of different vehicles and methods can be used for direct georeferencing of airborne imagery depending on the sensor and platform type. Today, differential kinematic GPS positioning is a standard tool for determining the camera exposure centres for aerial triangulation [Heipke et al, 2002]. Airborne GPS can greatly reduce, but not completely eliminate the need for ground control.

Since the need for GCP and overlapping imagery cannot be eliminated with the use of GPS, the integration of GPS and the inertial technology became a subject of research in this field. Inertial navigation relies on knowing the initial position of the object, velocity and attitude, and thereafter measuring the attitude rates and accelerations. An Inertial Navigation System (INS) consists of an Inertial Measurement Unit (IMU) or Inertial Reference Unit (IRU), and navigation computers to calculate the gravitational acceleration. However, in this report, the terms INS and IMU are used for the same purpose. An IMU is composed of gyroscopes, which is used for determining the rotation elements of the exterior orientation, and accelerometers, which provides the sensor velocity and position. In this report, use of the term INS is preferred. In principle, a GPS/IMU sensor combination can yield the exterior orientation elements of each image without aerial triangulation.

The application of direct georeferencing to the image data provides some important advantages, which can be summarized as:

- ◆ Direct georeferencing enables a faster acquisition of the exterior orientation, since the computational burden for automatic aerial triangulation is higher compared to the effort for GPS/inertial integration [Cramer, 1999].

- ◆ Direct georeferencing removes limitations to the flight path during image acquisition. Continuous absolute GPS trajectories, as obtainable by on-the-fly (OTF) methods, would in principle permit an aerial triangulation without ground control points. For that purpose a certain number of images has to be captured in the well-known photogrammetric block configuration. However, this flight configuration can be disadvantageous, if only small areas have to be captured or if a linear flight path is aspired for tasks like the supervision of power lines or the image acquisition at coast lines [Cramer, 1999].
- ◆ Additional problems of image matching required for automatic aerial triangulation are avoided if direct georeferencing is applied [Cramer, 1999].

Integrated systems will provide a system that has superior performance in comparison with either a GPS, an INS, or vision-based stand-alone system. The main strengths and weakness of INS and DGPS are summarized in figure 1.1.

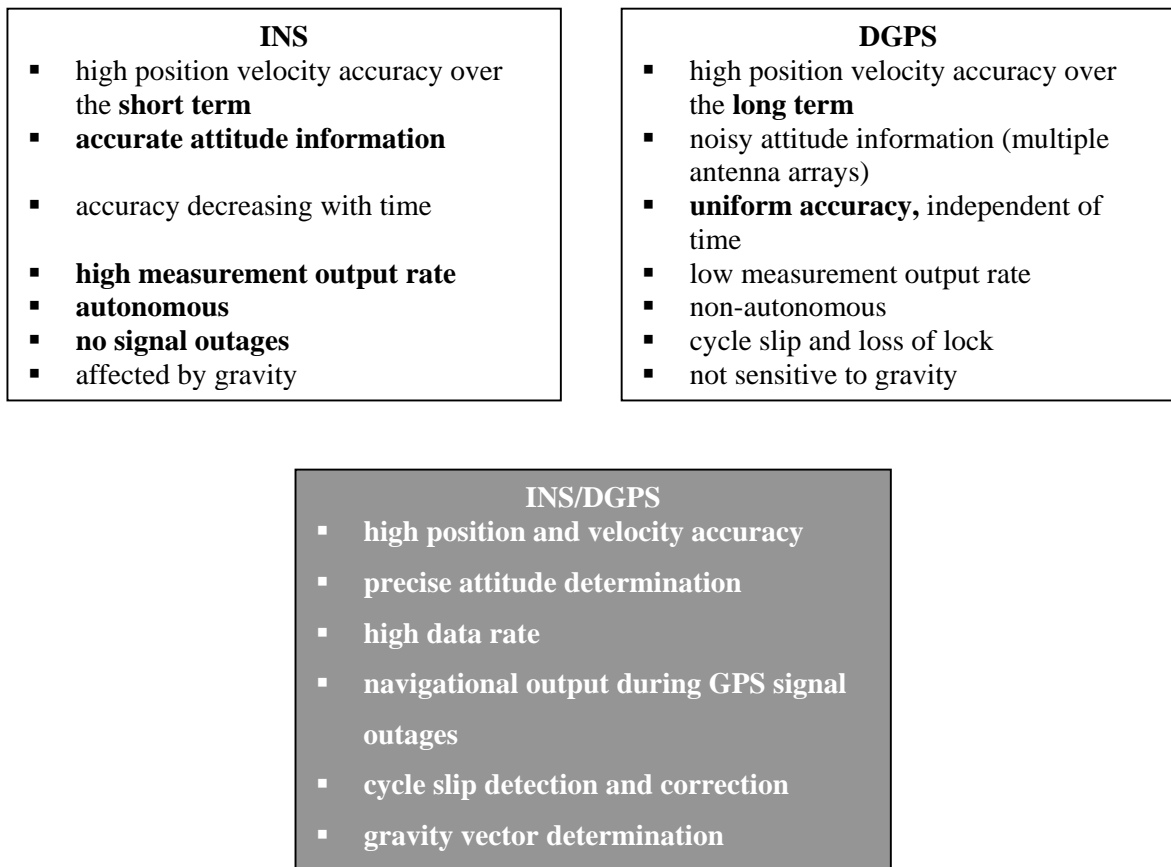


Figure 1.1: Benefits of INS/DGPS Integration [Skaloud, 1999].

The overall performance of the direct orientation method is limited primarily by the following components:

- ◆ Quality of the calibration of the integrated system:

- Imaging sensor modeling
- Lever arm between INS and GPS antenna
- Boresight transformation between INS and camera frames
- ◆ In-flight variation of the calibration components
- ◆ Rigidity of the imaging sensor/INS mount
- ◆ Quality of the IMU sensor
- ◆ Continuity of the GPS lock
- ◆ Kalman filter design [Grejner-Brzezinska, Toth, 2000].

Before using the position and orientation components (GPS antenna and IMU) for sensor orientation, we must determine the correct time, spatial eccentricity, and boresight alignment between the camera coordinate frame and IMU. The calibration of the GPS/IMU and the camera is vital since minor errors will cause major inaccuracies in object point determination [Sanchez, Hothem]. Direct georeferencing of airborne imaging data by INS/DGPS is schematically depicted in figure 1.2.

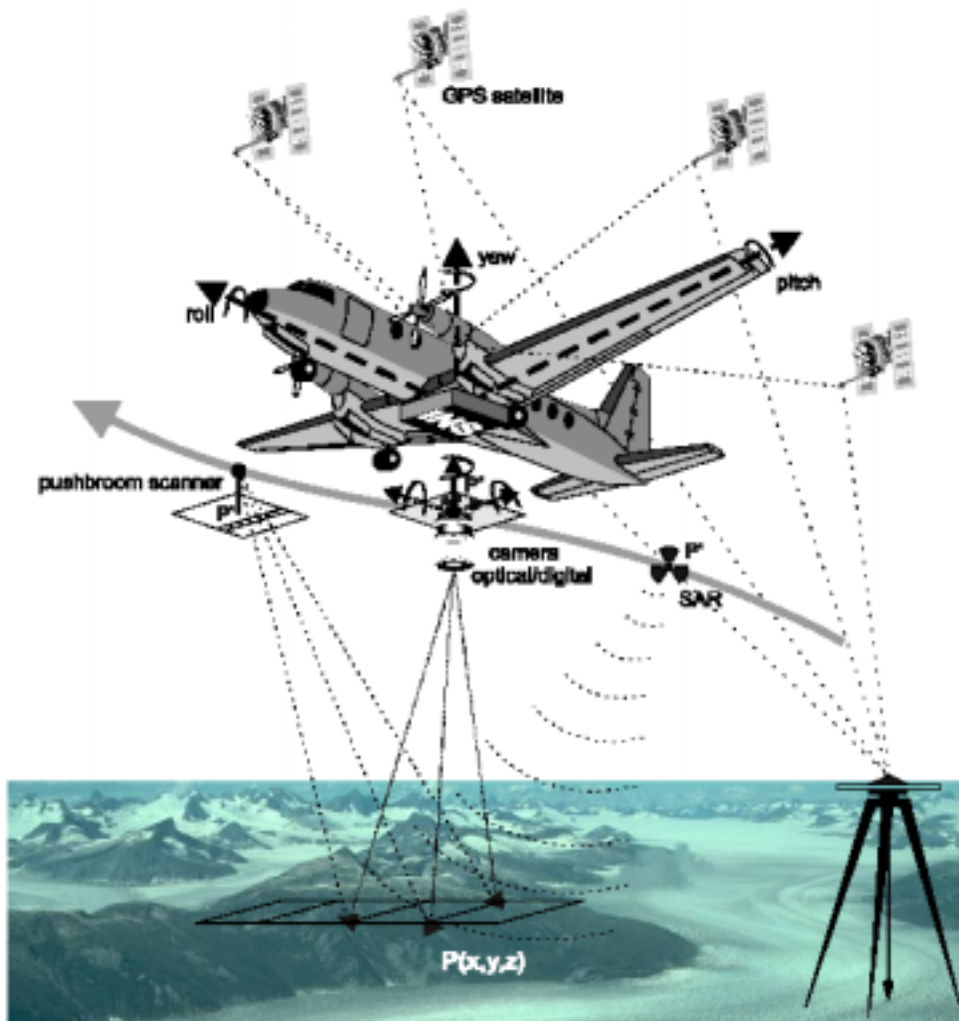


Figure 1.2: Direct georeferencing of airborne imaging by INS/DGPS [Skaloud, 1999].

Kalman Filter is an extremely effective and versatile procedure for *combining noisy sensor* outputs to estimate the *state of a system* with *uncertain dynamics*. In GPS/INS integration case, noisy sensors include GPS receivers and IMU components, and the system state include the position, velocity, acceleration, attitude, and attitude rate of a vehicle. Uncertain dynamics include unpredictable disturbances of the host vehicle and unpredictable changes in the sensor parameters [Grewal et al., 2001]. Kalman filter optimally estimates position, velocity, and attitude errors, as well as errors in the inertial and GPS measurements [Grejner-Brzezinska and Toth, 1998].

Main purposes of this report are to figure out basic system requirements of direct georeferencing of airborne imagery using GPS and INS, to explain the fundamentals of GPS/INS integration with Kalman Filtering and limitations of the integration, and to describe the common problems and results reported in the literature.

In the second and third parts of this report, the fundamentals and basic error models of GPS and INS are introduced, respectively. The theory of Kalman filtering for discrete and continuous processes are explained in the fourth part. While the integration purposes and types of GPS and INS are provided in the fifth part, a general overview of the applications seen in the literature is given in sixth part. The conclusion and future work is placed at the end of this report.

## **2 FUNDAMENTALS of the GPS**

The GPS, officially also known as NAVSTAR (Navigation and Satellite Timing and Ranging), is part of a satellite-based navigation system developed by the U.S. Department of Defense. GPS belongs to a large class of radio navigation systems that allow the user to determine his range and/or direction from a known signal transmitting station by measuring the differential time of travel of the signal. The Global Orbiting Navigation Satellite System (GLONASS) developed by Russia has almost an equivalent structure and used for satellite radio navigation purposes similar to GPS. Terrestrial radio navigation systems predate the satellite systems and include such as VOR (VHF Omnidirectional Range) and DME (Distance Measuring Equipment) for civilian aviation; the military equivalent, Tacan (Tactical Air Navigation); and low-frequency, long-range systems such as LORAN (Long Range Navigation) and OMEGA (Jekeli, 2000).

The GPS comprises a set of orbiting satellites at known locations in space and their signals can be observed on the Earth. Three distances to distinct satellites having known positions provide sufficient information to solve the observer's three-dimensional position. The system is designed so that a minimum of four satellites is always in view anywhere in the world to provide continual positioning capability. This is accomplished with 24 satellites distributed unevenly in six symmetrically arranged orbital planes.

The applications of GPS range from military navigation, vehicle monitoring, to sporting activities. For geodetic applications, the precise measurement of baselines (relative positioning) in static mode of GPS is widely used. Static positioning involves placing the receiver at a fixed location on the Earth and determining the position of that point. Opposite to this, kinematic positioning refers to determining the position of a vehicle or a platform that is moving continually with respect to Earth. It is also known as real-time positioning. The term navigation is used for real-time processing of the positioning data. Differential GPS (DGPS) is a technique for reducing the error in GPS-derived positions by using additional data from a reference GPS receiver at a known position. The most common form of DGPS involves determining the combined effects of navigation message ephemeris and satellite clock errors at a reference station and transmitting the pseudorange corrections in real time, to a user's receiver (Grewal et al., 2001).

The GPS is not without problems and limitations (Jekeli, 2000). It is not a self-contained, autonomous system. The user must be able to "see" the GPS satellites. Satellite visibility may be obstructed locally by intervening buildings, mountains, bridges, tunnels, etc. For kinematic applications, the effects of electronic interference or brief obstructions may cause the receiver to miss one or more cycles of the carrier wave. The frequency of the data output in most receivers is

often 1 Hz. Most of the error in GPS positioning come from medium propagation effects that are unpredictable to model such as atmospheric effects.

## 2.1 Clocks and Time

Each GPS satellite carries an atomic clock to provide timing information for the signals transmitted by the satellites. The clocks are oscillating at a particular frequency. The relationship between the phase  $\phi$ , frequency  $f$ , and the time is:

$$f(t) = \frac{d\phi(t)}{dt} \quad (2.1)$$

where  $t$  represents true time. The phase of an oscillating signal is the angle it sweeps out over time ( $0 \leq \phi \leq 2\pi$ ) and has the units of cycle. The frequency of the signal is the rate at which the phase changes in time and has the units of Hertz (cycles per second).

$$\phi(t) = \phi(t_0) + \int_{t_0}^t f(t') dt' \quad (2.2)$$

$t_0$  is some initial time.  $\tau$  denote the indicated time related to the phase:

$$\tau(t) = \frac{(\phi(t) - \phi_0)}{f_0} \quad (2.3)$$

$f_0$  is some nominal (constant) frequency since the initial indicated time does not coincide with initial phase ( $\phi(t_0) \neq \phi_0$ ).

The oscillator clock time ( $\tau$ ) and the true time ( $t$ ) differ from each other both in scale and in origin. The true time reflects the atomic clock time in U.S., which also differs from Coordinated Universal Time (UTC) by 2000 with 13 seconds. However, the GPS true time is calibrated by U.S. atomic time. The true time reflects the fact that the times indicated on satellite and receiver clocks are not perfectly uniform and must be calibrated by master clocks on the Earth. The relationship between the phase-time,  $\tau$ , and the true time,  $t$ , is:

$$\tau(t) = t - t_0 + \tau(t_0) + \delta\tau(t), \quad (2.4)$$

where,

$$\delta\tau(t) = \frac{1}{f_0} \int_{t_0}^t \delta f(t') dt'$$

The abbreviated form of (2.4) is:

$$\tau(t) = t - \Delta\tau(t) \quad (2.5)$$

## 2.2 GPS Signals

The signal is a carrier wave (sinusoidal wave) modulated in phase by binary codes that represent interpretable data. It can be represented mathematically by:

$$S(t) = AC(t)D(t)\cos(2\pi ft) \quad (2.6)$$

where  $f$  is the frequency of the carrier wave, and  $A$  is the amplitude of the signal. The code sequence  $C(t)$  is a step function having values (1, -1), also known as chips or bits.  $D(t)$  represents a data message.

Each satellite actually transmits two different codes, the C/A (coarse acquisition) code and the P-code (precision code). The P-code has 10 times higher chipping rate and wavelength in comparison with C/A code. They are transmitted on two separate microwave regions, an  $L_1$  signal with carrier frequency  $f_1 = 1545.72$  MHz and with wavelength  $\lambda_1 = 0.1903$  m; and an  $L_2$  signal with carrier frequency  $f_2 = 1227.6$  MHz and with wavelength  $\lambda_2 = 0.2442$  m. The transmission on two frequencies allows approximate computation of the delay of the signal due to ionospheric refraction. The total signal transmitted by the satellite is given by the sum of three sinusoids, two for the two codes on the  $L_1$  carrier and one for the P-code on the  $L_2$  carrier. The total signal transmitted by a GPS satellite is given by

$$S^P(t) = A_P P^P(t) W^P(t) D^P(t) \cos(2\pi f_1 t) + A_C C^P(t) D^P(t) \sin(2\pi f_1 t) + B_P P^P(t) W^P(t) D^P(t) \sin(2\pi f_2 t) \quad (2.7)$$

$A_P$ ,  $A_C$ , and  $B_P$  represent amplitudes of the corresponding codes, C and P represent C/A and P codes, D represents the data message, superscript P identifies a particular satellite, and W represents a special code which is used to decrypt a military code.

The codes serve two operational purposes: determining the range between the satellite and receiver and to spread the signal over a large frequency bandwidth, thus permitting small antennas on the Earth to gather the transmitted signal. Both codes consist of unique sequences of binary states that are generated using a pseudorandom noise (PRN) algorithmic process. The PRN for C/A code is different for each satellite and repeats every millisecond. For P-code, it is much longer and repeats only after 38 weeks. Each satellite uses only one distinct week's worth of the code. The satellites are distinguished by the codes rather than by frequency.

### 2.3 GPS Receiver

Before the signal is processed by the receiver, it is pre-amplified and filtered at the antenna, and subsequently down-shifted in frequency to a more manageable level for processing (Jekeli, 2000). The mixed signal is given by

$$\begin{aligned}
 S_r(t) S^P(t) &= A \cos(2\pi f_{LO}t) \cos(2\pi f_s t + \phi(t)) \\
 &= \frac{A}{2} \cos(2\pi(f_s - f_{LO})t + \phi(t)) + \frac{A}{2} \cos(2\pi(f_s + f_{LO})t + \phi(t))
 \end{aligned}
 \tag{2.8}$$

where  $S_r(t)$  is the pure signal sinusoid generated by the receiver oscillator,  $f_{LO}$  is the local oscillator frequency,  $S^P(t)$  is the satellite signal with frequency  $f_s$ , and  $A$  is an amplitude factor.

The satellite signal is then shifted to an intermediate frequency (IF), and appropriate filters are applied to control the amplitude of the signal for subsequent processing. The signal then passes to the main signal processing part of the receiver.

To calculate the distance between the satellite and the receiver, the time tag of the signal at the time of transmission and the time of reception at the receiver is compared, and using the speed of the light, the delay is converted to the distance. It is not the true range if the satellite and the receiver clocks differ; and therefore, the calculated range is called *pseudorange*.

### 2.4 GPS Observables and Errors

A broad overview of GPS errors is provided in table 2.1. The largest error is due to the receiver clock. The next significant error source is the medium in which the signal must travel. This includes the Ionosphere, which has an altitude between 50 km to 1000 km and has many free electrons; and the Troposphere, which is a non-dispersive medium and contains mostly electrically neutral particles.

Table 2.1: Error sources in GPS positioning (Jekeli, 2000).

Error Source	Typical Magnitude
Receiver clock error (synchronized)	1 $\mu$ s (300 m)
Residual satellite clock error	20 ns (6m)
Satellite synchronization to UTC	100 ns (30 m)
Selective Availability (cancelled by 2001)	100 m

Orbit error (precise, IGS)	20 cm
Tropospheric delay	<30 m
Ionospheric delay	<150 m
Multipath	<5 m (P-code); <5 cm (phase)
Receiver Noise	1 m (C/A code); 0.1 m (P-code); 0.2 mm (L <sub>1</sub> phase)

Other errors in GPS observables include the multipath error (the reflection of the GPS signal from nearby objects prior to entering the antenna), equipment delays and biases, antenna eccentricities (phase center variations), and the thermal noise of the receiver.

The pseudorange is formulated as

$$S_r^P(\tau_r) = \rho_r^P(\tau_r) + c(\Delta \tau_r(t) - \Delta \tau^P(t - \Delta t_r^P)) + \Delta \rho_{iono,r}^P + \varepsilon_{\rho,r}^P \quad (2.9)$$

where  $\rho_r^P(\tau_r)$  is the true range between the satellite and the receiver,  $\Delta t_r^P$  is the time of transit,  $\Delta \rho_{iono,r}^P$  is the ionospheric error for each satellite,  $c$  is the speed of the light, and  $\varepsilon_{\rho,r}^P$  represents pseudorange observation error (different for each satellite). For simplicity, the Tropospheric delay, the equipment and antenna offsets, the multipath error, and the time registration error due to the receiver clock error are excluded.

The phase observable can be expressed as follows:

$$\phi_r^P(\tau_r) = \frac{f_0}{c} \rho_r^P(\tau_r) + f_0(\Delta \tau_r(t) - \Delta \tau^P(t - \Delta t_r^P)) + \phi_{0,r} - \phi_0^P - N_r^P + \Delta \phi_{iono,r}^P + \varepsilon_{\phi,r}^P \quad (2.10)$$

where  $\phi_{0,r}$  and  $\phi_0^P$  are the arbitrary phase offsets,  $N_r^P$  is the integer representing the unknown number of full cycles and also called as carrier phase ambiguity,  $\varepsilon_{\phi,r}^P$  is the phase observation error.

## 3 FUNDAMENTALS of INERTIAL NAVIGATION

### 3.1 Basic Concepts of Inertial Navigation

*Inertia* is the propensity of bodies to maintain constant translational and rotational velocity, unless disturbed by forces or torques, respectively (Newton's first law of motion). An *inertial reference frame* is a coordinate frame which Newton's law of motion are valid. Inertial reference frames are neither rotating nor accelerating (Grewal et al., 2001). *Inertial sensors* measure rotation rate and acceleration by *gyroscopes* and *accelerometers* respectively. Accelerometers cannot measure gravitational acceleration, which is an accelerometer in free fall or in orbit has no detectable input. The *input axis* of an inertial sensor defines which vector component it measures. Multi-axis sensors measure more than one component.

*Inertial navigation* uses gyroscopes and accelerometers to maintain an estimate of the position, velocity, attitude, and attitude rates of the vehicle in or on which the INS is carried. An INS consists of *navigation computers*, to calculate the gravitational acceleration and to integrate the net acceleration, and an *inertial measurement unit* containing accelerometers and gyroscopes.

Literally, there are thousands of designs for gyroscopes and accelerometers. Not all of them are used for inertial navigation. For example, gyroscopes are used for steering and stabilizing ships, missiles, cameras and binoculars, etc. The acceleration sensors are also used for measuring gravity, sensing seismic signals, leveling, and measuring vibrations.

Traditionally, inertial systems have been divided into three groups according to the free-running growth of their position error (Skaloud, 1999):

- the strategic-grade instruments ( performance  $\approx 100$  ft/h)
- the navigation-grade instruments (performance  $\approx 1$  nm/h)
- the tactical-grade instruments (performance  $\approx 10$ -20 nm/h)

In a further categorization, the inertial navigation systems are designed in two main groups: the *platform* (or *gimbaled*) systems and the *strapdown* systems. In a gimbaled system the accelerometer triad is rigidly mounted on the inner gimbal of three gyros (see figure 3.1.b). The inner gimbal is isolated from the vehicle rotations and its attitude remains constant in a desired orientation in space during the motion of the system. The gyroscopes on the stable platform are used to sense any rotation of the platform, and their outputs are used in servo feedback loops with gimbal pivot torque actuators to control the gimbals such that the platform remains stable. These

systems are very accurate, because the sensors can be designed for very precise measurements in a small measurement range.

In contrary, a strap-down inertial navigation system uses orthogonal accelerometers and gyro triads rigidly fixed to the axes of the moving vehicle (figure 3.1.a). The angular motion of the system is continuously measured using the rate sensors. The accelerometers do not remain stable in space, but follow the motion of the vehicle.

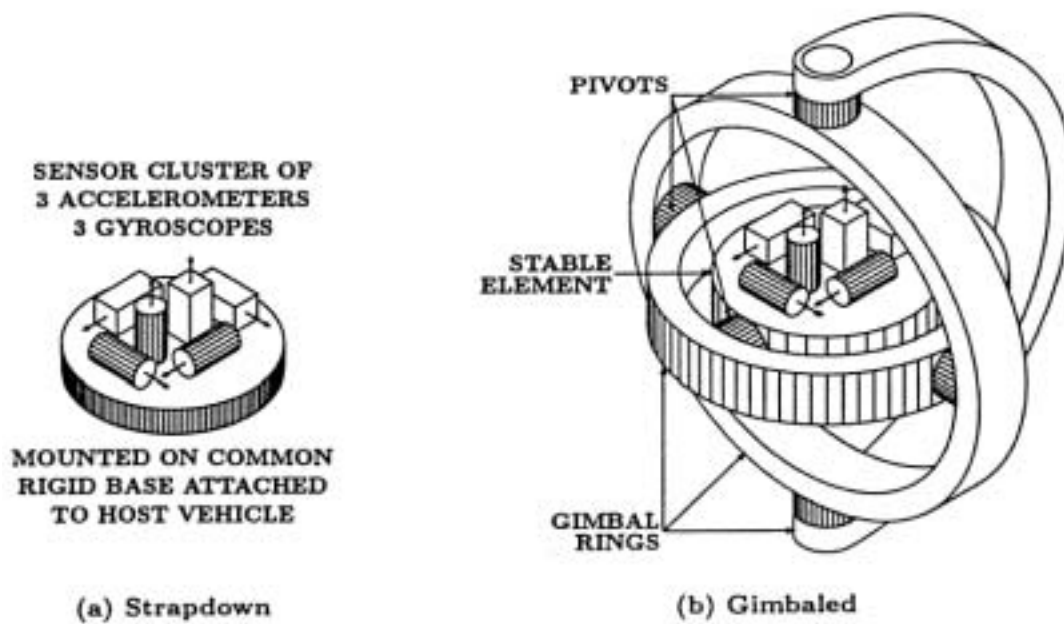


Figure 3.1: Inertial measurement units (Grewal et al., 2001).

### 3.2 Common Sensor Error Models

Gyroscopes, which are used as attitude sensors in inertial navigation, are also called as inertial grade. There are many types of gyroscope designs, such as momentum wheels, rotating multisensor, laser gyroscopes, etc. Error models for gyroscopes are primarily used for two purposes: predicting performance characteristics as function of gyroscope design parameters and calibration and compensation of output errors. The common error sources for gyroscopes are output bias, input axis misalignments, combined (clustered) three-gyroscope compensation, input/output non-linearity, and acceleration sensitivity.

Depending on the purpose, acceleration sensors also have several designs such as, gyroscopic accelerometers, pendulous accelerometers, strain-sensing accelerometers, etc. The main error sources for accelerometers are biases, parameter instabilities (i.e., turn-on and drift), centrifugal

acceleration effects due to high rotation rates, center of percussion, and angular accelerometer sensitivity.

### **3.3 Initialization and Alignment**

INS initialization is the process of determining initial values for system position, velocity, and attitude in navigation coordinates. INS position initialization ordinarily relies on external sources such as GPS or manual entry. INS velocity initialization can be accomplished by starting when it is zero (i.e., the host vehicle is not moving) or by reference to the carrier velocity.

INS alignment is the process of aligning the stable platform axes parallel to navigation coordinates (for gimballed systems) or that of determining the initial values of the coordinate transformation from sensor coordinates to navigation coordinates (for strapdown systems). There are four basic methods for INS alignment (Grewal et al., 2001):

- i) Optical alignment using either optical line-of-sight reference to a ground based direction or an on board star tracker.
- ii) Gyrocompass alignment of stationary vehicles, using the sensed direction of acceleration to determine the local vertical and sensed direction of rotation to determine north.
- iii) Transfer alignment in a moving host vehicle, using velocity matching with an aligned and operating INS.
- iv) GPS-aided alignment, using position matching with GPS to estimate the alignment variables.

### **3.4 System-Level Error Models**

Since there is no single, standard design for an INS, the system-level error sources vary very much. General error sources can be classified as:

- i) initialization errors, comes from initial estimates of position and velocity;
- ii) alignment errors, from period for initial alignment of gimbals or attitude direction cosines (for strapdown systems) with respect to navigation axes;
- iii) sensor compensation errors, occur due to the change in the initial sensor calibration over the time;
- iv) gravity model errors, is the influence of the unknown gravity modeling errors on vehicle dynamics.

## 4 KALMAN FILTERING BASICS

Within the significant toolbox of mathematical tools that can be used for stochastic estimation from noisy sensor measurements, one of the most well known and often-used tools is what is known as the *Kalman Filter*. The Kalman filter is named after Rudolph E. Kalman, who in 1960 published his famous paper describing a recursive solution to the discrete-data linear filtering problem (Kalman, 1960). The Kalman Filter is essentially a set of mathematical equations that implement a predictor-corrector type estimator that is *optimal* in the sense that it minimizes the estimated *error* covariance—when some presumed conditions are met. Since the time of its introduction, the *Kalman Filter* has been the subject of extensive research and application, particularly in the area of autonomous or assisted navigation.

Basically, Kalman Filter is a special case of sequential least square estimation, where initial measurement is equal to the first measurement and design matrix of the second position is an identity matrix. Kalman Filter also takes the velocity as an unknown parameter. Three sequential algorithms; Triangular Factor Update (TFU) with Gauss/Cholesky decompositions, Givens Update and Kalman Update for photogrammetric processing of images were emphasized by Gruen (1984) and Gruen and Kersten (1992). For more detailed information on least squares filtering of dynamic linear systems and Kalman filtering, see Gelb (1974), and Salzmann (1993).

### 4.1 Discrete Kalman Filter

Basic concepts of random processes can be found in the appendix. The Kalman Filter addresses the general problem of trying to estimate the state  $x \in \mathfrak{R}^n$  of a discrete-time controlled process that is governed by the linear stochastic difference equation

$$x_k = Ax_{k-1} + Bu_k + w_{k-1} \quad (4.1)$$

with a measurement  $z \in \mathfrak{R}^m$  that is

$$z_k = Hx_k + v_k \quad (4.2)$$

The random variables  $w_k$  and  $v_k$  represent the process and measurement noise (respectively). They are assumed to be independent (of each other), white, and with normal probability distributions

$$p(w) \sim N(0, Q) \quad (4.3)$$

$$p(v) \sim N(0, R) \quad (4.4)$$

In practice,  $A$ , the process noise covariance  $Q$ , and measurement noise covariance  $R$  matrices might change with each time step. However, here, they are assumed to be constant.

Let's define  $\hat{x}_k^- \in \mathcal{R}^n$  as a priori state estimate at step k given the knowledge of the process prior to step k, and  $\hat{x}_k \in \mathcal{R}^n$  as a posteriori state estimate at step k given the measurement  $z_k$ . A priori and a posteriori estimate errors and error covariances are:

$$\begin{aligned} e_k^- &\equiv x_k - \hat{x}_k^-, & P_k^- &= E[e_k^- e_k^{-T}] \\ e_k &\equiv x_k - \hat{x}_k, & P_k &= E[e_k e_k^T] \end{aligned}$$

The linear combination between a posteriori state estimate  $\hat{x}_k$ , a priori state estimate  $\hat{x}_k^-$ , and a weighted difference between an actual measurement  $z_k$  and measurement prediction  $H \hat{x}_k^-$  is:

$$\hat{x}_k = \hat{x}_k^- + K(z_k - H \hat{x}_k^-) \quad (4.5)$$

In the equation,  $(z_k - H \hat{x}_k^-)$  is called measurement innovation or the residual. K matrix is also called as Kalman gain matrix and can be shown as:

$$K_k = P_k^- H^T (H P_k^- H^T + R)^{-1} \quad (4.6)$$

The Kalman Filter estimates a process by using a form of feedback control: the filter estimates the process state at some time and then obtains feedback in the form of (noisy) measurements. As such, the equations for the Kalman Filter fall into two groups: time update equations and measurement update equations. The time update equations are responsible for projecting forward (in time) the current state and error covariance estimates to obtain the a priori estimates for the next time step. The measurement update equations are responsible for the feedback—i.e. for incorporating a new measurement into the a priori estimate to obtain an improved a posteriori estimate (Welch and Bishop, 2002). After each time and measurement update pair, the process is repeated with the previous a posteriori estimates used to project or predict the new a priori estimates in recursive nature (figure 4.1).

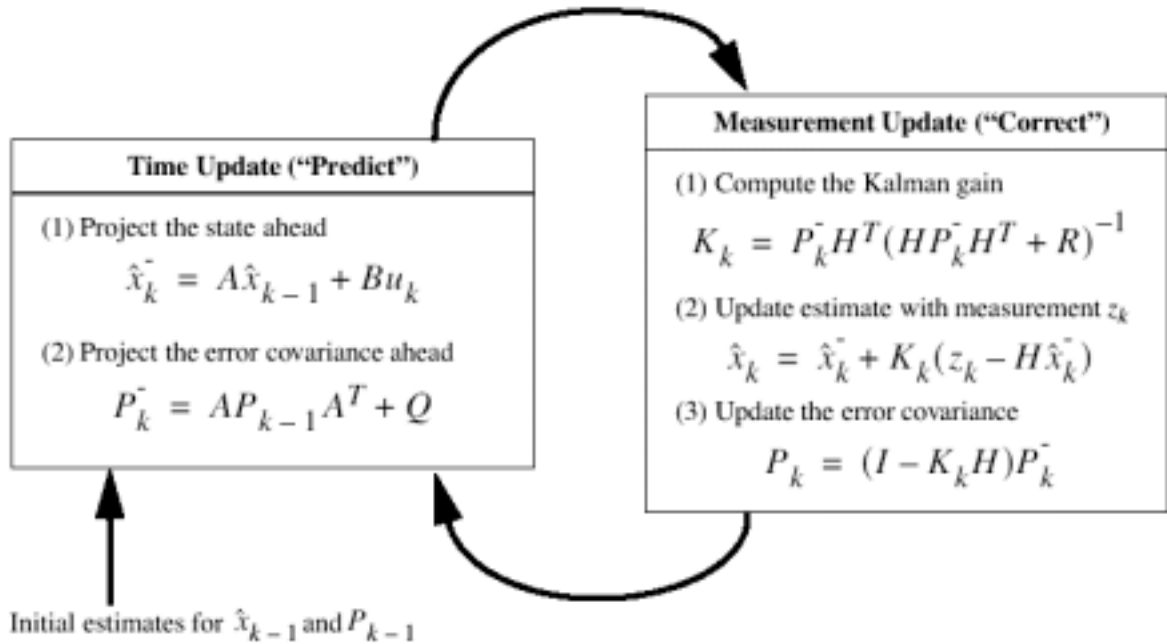


Figure 4.1: A complete picture of the Kalman Filter (Welch and Bishop, 2002).

## 4.2 The Extended Kalman Filter

Extended Kalman Filter (EKF) linearizes the current mean and covariance when the process to be estimated or the related measurement is non-linear. The stochastic difference equation of the state vector  $x \in \mathfrak{R}^n$  of the non-linear process is defined as:

$$x_k = f(x_{k-1}, u_k, w_{k-1}) \quad (4.7)$$

with a measurement  $z \in \mathfrak{R}^m$  that is

$$z_k = h(x_k, v_k) \quad (4.8)$$

where the random variables  $w_k$  and  $v_k$  represent the process and measurement noise. We can approximate the state and measurement vectors as:

$$\tilde{x}_k = f(\hat{x}_{k-1}, u_k, 0) \quad (4.9)$$

$$\tilde{z}_k = h(\tilde{x}_k, 0) \quad (4.10)$$

where  $\hat{x}_k$  is a posteriori estimate of the state. The actual state and measurement vectors related with the approximated state and measurement vectors are:

$$x_k \approx \tilde{x}_k + A(x_{k-1} - \hat{x}_{k-1}) + Ww_{k-1} \quad (4.11)$$

$$z_k \approx \tilde{z}_k + H(x_k - \tilde{x}_k) + Vv_k \quad (4.12)$$

where;

$$A_{[i,j]k} = \frac{\partial f^{[i]}}{\partial x^{[j]}}(\hat{x}_{k-1}, u_k, 0) \quad (4.13)$$

$$W_{[i,j]k} = \frac{\partial f^{[i]}}{\partial w^{[j]}}(\hat{x}_{k-1}, u_k, 0) \quad (4.14)$$

$$H_{[i,j]k} = \frac{\partial h^{[i]}}{\partial x^{[j]}}(\tilde{x}_k, 0) \quad (4.15)$$

$$V_{[i,j]k} = \frac{\partial h^{[i]}}{\partial v^{[j]}}(\tilde{x}_k, 0) \quad (4.16)$$

The definitions of the prediction error and measurement residual are respectively:

$$\tilde{e}_{x_k} \equiv x_k - \tilde{x}_k \approx A(x_{k-1} - \hat{x}_{k-1}) + \varepsilon_k \quad (4.17)$$

$$\tilde{e}_{z_k} \equiv z_k - \tilde{z}_k \approx H\tilde{e}_{x_k} + \eta_k \quad (4.18)$$

where  $\varepsilon_k$  and  $\eta_k$  represent new independent random variables having zero mean and covariance matrices and, with and as in  $WQW^T$  and  $VRV^T$ , with  $Q$  and  $R$  as in (4.3) and (4.4) respectively.

The equations (4.17) and (4.18) are linear, and they are similar to the equations (4.1) and (4.2) from Discrete Kalman Filter. A second (hypothetical) Kalman Filter can be used with the actual measurement residual  $\tilde{e}_{z_k}$  in equation (4.18) and the prediction error to  $\tilde{e}_{x_k}$  given by equation

(4.17) to estimate  $\hat{e}_k$  which can be used to obtain the a posteriori estimates for the original non-linear process as:

$$\hat{x}_k = \tilde{x}_k + \hat{e}_k \quad (4.19)$$

The random variables of equations (4.17) and (4.18) have approximately following probability distributions:

$$p(\tilde{e}_{x_k}) \sim N(0, E[\tilde{e}_{x_k} \tilde{e}_{x_k}^T])$$

$$p(\epsilon_k) \sim N(0, WQ_k W^T)$$

$$p(\eta_k) \sim N(0, VR_k V^T)$$

Given these approximations and letting the predicted value of  $\hat{e}_k$  be zero, the Kalman Filter equation used to estimate  $\hat{e}_k$  is:

$$\hat{e}_k = K_k \tilde{e}_{z_k} \quad (4.20)$$

By substituting equation (4.20) back into equation (4.19) and making use of equation (4.18) we get:

$$\begin{aligned} \hat{x}_k &= \tilde{x}_k + K_k \tilde{e}_{z_k} \\ &= \tilde{x}_k + K_k (z_k - \tilde{z}_k) \end{aligned} \quad (4.21)$$

Equation (4.21) now can be used for the measurement update in the extended Kalman Filter. A complete set of EKF equations is shown in figure 4.2. The term  $\tilde{x}_k$  is substituted with  $\hat{x}_k^-$  to be consistent with Discrete Kalman Filter equations.

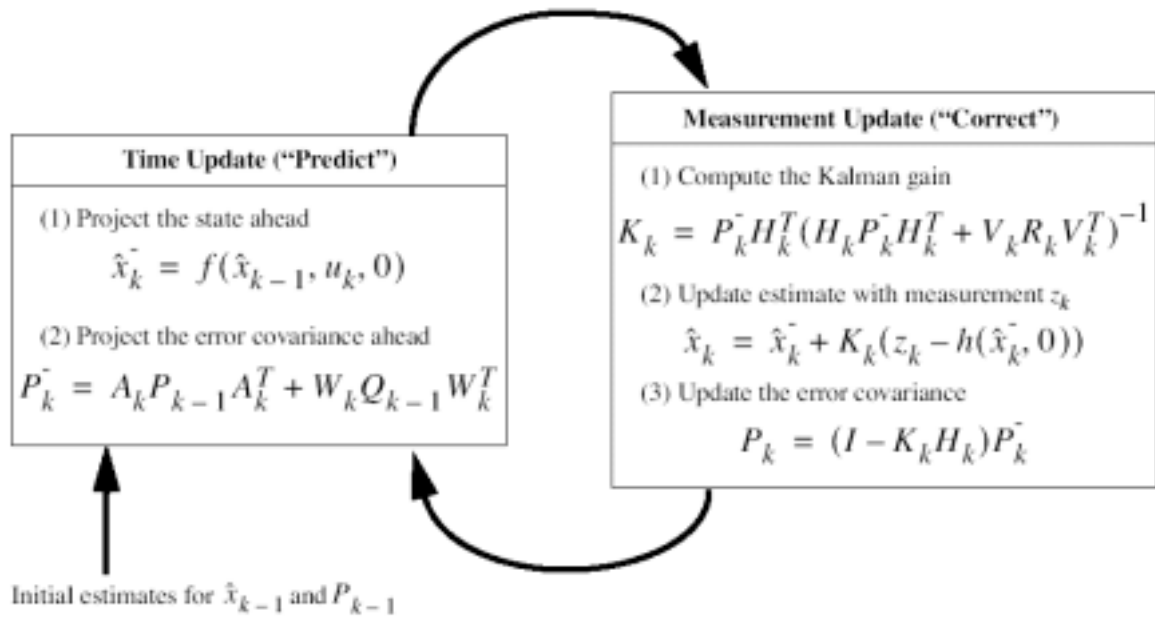


Figure 4.2: A complete picture of the operation of the *extended* Kalman filter (Welch and Bishop, 2002).

## 5 GPS and INS INTEGRATION

The Galileo's Law,  $\delta x = 0.5 \delta a t^2$ , illustrates the position prediction precision of a moving platform, where  $\delta x$ ,  $\delta a$ , and  $t$  represent variation in position, change in acceleration, and the time interval respectively. The relatively low data output rate of GPS receivers (usually 1 Hz) might not meet the cm level accuracy requirements of aerial photogrammetry. This problem becomes more serious when the potential temporarily loss of a GPS signal occurs or phase ambiguity resulting from cycle slips considered. INS provides the dynamics of motion between GPS epochs at high temporal resolution and complements the discrete nature of GPS in the occurrence of cycle slips or signal loss.

In addition, positioning with INS requires the integration with respect to time of accelerations and angular rates, the measurement noise accumulates and results in long wavelength errors. GPS errors do not accumulate, but in short term, they are relatively larger and the measurements have poorer resolution. INS is an autonomous system, except the initialization requirements, and do not ask for external support.

Due to the complementary nature of both system, the integrated GPS/INS has become widely used positioning purposes, especially on mobile mapping systems. The integrated systems are in use on different platforms, such as aircrafts, ground vehicles, satellites, etc. Several systems have been developed around the world.

When the navigation information is provided by an integrated INS/DGPS system, the equation of direct georeferencing for aerial frame cameras takes the form:

$$r_i^m = r_{ins/dgps}^m(t) + R_b^m(t)[s_i R_c^b r_i^c(t) + a^b] \quad (5.1)$$

where,

$r_i^m$  is coordinate vector of a specific point ( $i$ ) in the mapping frame,

$r_{ins/dgps}^m(t)$  is coordinate vector of INS center in the mapping frame, determined by INS/DGPS integration,

$R_b^m(t)$  is the attitude matrix from INS body frame to the mapping frame, , determined by INS/DGPS integration,

$s_i$  is a scale factor between the image and mapping coordinate frames for a specific point ( $i$ ), usually determined by processing the captured imagery in stereo pairs,

$R_c^b$  is the rotation matrix (orientation offset) between the camera frame and the INS body frame determined from calibration,

$r_i^c(t)$  is the vector of coordinates (i.e., x, y, -f) observed in the image frame for a specific image ( $t$ ) and point ( $i$ ),

$a^b$  is the vector of the translation offset between the INS and the camera centre in the INS body frame determined by terrestrial measurements as part of the calibration process (Skaloud, 1999).

However, some small changes should be done in this equation when pushbroom cameras or other applications such SAR are considered. For SAR applications, see Dowman (1995) for laser applications see Favey et al. (1999).

## 5.1 Integration Modes

The types of integration can be categorized by the extent to which data from each component aid the other's function. First one is coupling of the systems and depends on the mechanization or the architecture of the system. The second categorization parameter is by the method of combining or fusing the data to obtain position coordinates.

The system mechanization is generally understood in two ways, tight coupling and loosely coupling; where no coupling implies no data feedback from either instrument to the other for the purpose of improving its performance. Tightly coupled sensors are treated as belonging to a single system producing complementary types of data. The produced data are produced simultaneously and optimally, and used to enhance the function of individual sensor components where possible. In a loosely coupled system, processed data from one instrument are fed back in an aiding capacity to improve the utility of the other's performance, but each instrument still has its own individual data processing algorithm.

The real-time feedback of INS velocities to the GPS receiver enables an accurate prediction of GPS pseudorange and phase at next epoch, thus allowing a smaller bandwidth of the receiver tracking loop in a high-dynamic environment with a subsequent increase in accuracy. Conversely, inertial navigation improves if the GPS solution functions as an update in a Kalman filter estimation of the systematic errors in the inertial sensors. Similarly, GPS positions and velocities may be used to aid the INS solution in a high-dynamic situation by providing a better reference for propagating error states based on the linear approximation. (Jekeli, 2000)

There are two basic categories of processing algorithms that are centralized and de-centralized. In centralized processing, the raw sensor data is combined optimally using one central processor to obtain a position solution. This kind of processing is usually associated with tight system integration. Decentralized processing is a sequential approach to processing, where processors of individual systems provide solutions that subsequently are combined with various degrees of optimality by a master processor. In principle, if the statistics of the errors are correctly propagated,

the optimal decentralized and centralized methods should yield identical solutions (Jekeli, 2000). In some certain cases, such as system fault detection, isolation, and correction capability and the relative computational simplicity makes the decentralized approach more favourable. The centralized approach provides the best performance in navigation solutions that a single robust Kalman filter model. Different forms of integration are evaluated in table 5.1.

Table 5.1: Different forms of Kalman filter implementation (Skaloud, 1999).

<i>Implementation</i>	<i>Advantages</i>	<i>Disadvantages</i>
Open loop	<ul style="list-style-type: none"> <li>• KF may be run external to INS, suitable for platform INS</li> <li>• Used when only navigation solution from INS available</li> </ul>	<ul style="list-style-type: none"> <li>• Non-linear error model due to large second-order effect</li> <li>• Extended KF needed</li> </ul>
Closed loop	<ul style="list-style-type: none"> <li>• Inertial system errors, linear model is sufficient</li> <li>• Suitable for integration at software level</li> </ul>	<ul style="list-style-type: none"> <li>• More complex processing</li> <li>• Blunders in GPS may affect INS performance</li> </ul>
Loosely coupled (decentralized)	<ul style="list-style-type: none"> <li>• Flexible, modular combination</li> <li>• Small KF, faster processing</li> <li>• Suitable for parallel processing</li> </ul>	<ul style="list-style-type: none"> <li>• Sub-optimal performance</li> <li>• Unrealistic covariance</li> <li>• Four satellites needed for a stable solution</li> <li>• INS data not used for ambiguity estimation</li> </ul>
Tightly-coupled (centralized)	<ul style="list-style-type: none"> <li>• One error state model</li> <li>• Optimal solution</li> <li>• GPS measurements can be used with less than 4 satellites</li> <li>• Direct INS aiding throughout GPS outages</li> <li>• Faster ambiguity estimation.</li> </ul>	<ul style="list-style-type: none"> <li>• Large size of error state model</li> <li>• More complex processing</li> </ul>

The vector state estimation can be implemented in open or closed, whether the estimated sensor errors are fed back to correct the measurements. When properly designed, the closed-loop implementation generally has better performance and is therefore the preferred implementation when using a strapdown INS. The loosely-coupled filtering approach has been highly popular due its modularity and smaller filter size. Although the arguments for choosing either form of the implementation have been very balanced, the tightly-coupled approach is currently gaining more weight mainly due to the rapid increase in computational power (Skaloud, 1999).

## 5.2 Integration Limitations

The performance of an integrated INS/DGPS is a complex process depending on a variety of parameters including

- quality and type of inertial sensors
- the baseline length

- operational aspects
- the validity of error models
- the estimation algorithm. (Skaloud, 1999)

The improvements in trajectory determination are usually sought in the development of better models and estimation algorithms. With the rapid increase of computational power, the trend of finding the most suitable error model for a specific system and specific conditions is being replaced by using a multi-model approach in conjunction with some type of adaptive estimation. Another limiting factor band frequency. In the lower frequencies, the INS/DGPS integration reduces the overall error; and in the high frequencies, the overall error is not reduced (Skaloud, 1999).

## **6 A SPECIAL APPLICATION AREA: DIRECT GEOREFERENCING of AIRBORNE IMAGERY**

In the literature, there are several system designs for georeferencing of airborne images; and regarding to these designs, different integration methods are proposed. In general, strapdown INSs are preferred due to its low-cost character. The trend is tending to implementation of integration methods for low-cost IMU and most of the applications are in this manner. However, different systems ask for different accuracies. A brief overview of accuracy requirements for different applications areas can be found in Schwarz et al (1994), and Schwarz (1995).

In the University of Calgary the INS/GPS integration strategies are analyzed and different design methods for several system implemetations are suggested. The results of two different implementations, a low-cost system and a high-cost navigation grade system, using strapdown INSs are presented by Schwarz (1995). Error models for INS/GPS integration and design methods for improving attitude accuracy are discussed by Skaloud and Schwarz (2000).

Skaloud (1999) developed a Kalman filtering method for optimizing the airborne survey systems by INS/DGPS. The centralized and decentralized approaches are compared with respect to on-the-fly (OTF) GPS ambiguity estimation. In this work, the operational procedures; such as sensor placement, effect of vibrations, alignment of the inertial system, sensor synchronization and calibration; are investigated to eliminate or substantially reduce error sources of the integrated system. A strapdown INS, dual frequency GPS receivers, and a frame aerial camera are used for demonstration of the developed method in a test project with 47 GCPs and image scale 1/6000. As a result, 15-20 cm and 20-25 cm planimetry and height positioning accuracies are gathered with and without using GCPs, respectively. Although the decentralized approach gives the flexibility of INS selection, since the centralized Kalman Filtering increases the probability of resolving ambiguities faster and with fewer satellites as compared to its decentralized counterpart, this form of filtering is recommended for direct georeferencing by INS/DGPS. The imaging sensor is recommended to be mounted together with the inertial system on a common, solid structure connected to the aircraft via vibration absorbers. The spatial distance between individual sensors are advised to be kept as small as possible. Also, inflight alignment is recommended over the static alignment due to better time efficiency when using INS.

The European Organisation for Experimental Photogrammetric Research (OEEPE) has embarked on a multi-site test investigating sensor orientation using GPS and IMU in comparison and in combination with aerial triangulation. The focus of the test was on the obtainable accuracy for large

scale topographic mapping using photogrammetric film cameras. The accuracy of the results was assessed with the help of independent check points on the ground in the following scenarios:

- conventional aerial triangulation,
- GPS/IMU observations for the projection centres only (direct sensor orientation),
- combination of aerial triangulation with GPS/IMU (integrated sensor orientation) (Heipke et al., 2002).

For the test, an aerial film camera is used in a test flight with image scale 1/5000. GPS data are acquired by dual frequency GPS receivers using differential carrier phase measurements with a data rate of 2 Hz preferably with identical receivers for the aircraft and reference station. A short base line between aircraft and reference station was set. A high quality off-the-shelf navigation grade IMU as typically used in precise airborne attitude determination was also established. The accuracy potential of direct sensor orientation as determined from the best results lies at approximately 5-10 cm in planimetry and 10-15 cm in height when expressed as RMS differences at independent check points, and at 15-20  $\mu\text{m}$  when expressed as  $\sigma_0$  values of the over-determined forward intersection in image space. These values are larger by a factor of 2-3 when compared to standard photogrammetric results. The maximum errors are in the range of 30-50 cm. When the results of integrated sensor orientation are compared to direct sensor orientation, the a posteriori standard deviation of the image coordinates  $\sigma_0$  is greatly reduced. This finding confirms the expectations that a local refinement of the image orientation is achieved by introducing tie points.  $\sigma_0$  is in the same range as for the photogrammetric reference solutions. Consequently, integrated sensor orientation does allow for stereo plotting in the same way as conventional photogrammetry. In planimetry the RMS differences in object space are only slightly better than in the case of direct sensor orientation. Improvements have primarily occurred in height (Heipke et al., 2002).

A digital Airborne Integrated Mapping System (AIMS) for large-scale mapping and other precise positioning applications is being developed in the Center for Mapping in Ohio State University (Grejner-Brzezinska and Toth, 1998). A medium accuracy strapdown INS is tightly integrated with the GPS on an aerial platform. By the authors, AIMS is the first tightly integrated system which provides sub-decimeter accuracy for large-scale applications. A frame CCD camera is used on the platform. The system architecture of AIMS is given in figure 6.1. A closed-loop Kalman filtering method is also used for the integration. A single Kalman Filter, with number of states equal to 21 plus the number of double differences, is used to process the GPS double-differenced phases, combined with the inertial solution. The state unknowns are errors in position, velocity, and orientation, three biases and three scale factors for the accelerometers, three gyro drifts, two deflections of the vertical and the gravity anomaly. In addition, GPS ionospheric delay is estimated for every satellite in the solution (table 6.1). The first performance test results are provided by Toth

and Grejner-Brzezinska (1998) for an image scale of 1/2400. The coordinate differences between GPS/INS positions and aerotriangulation are around 15 cm in both horizontal and vertical directions. The system calibration issues for AIMS and a performance analysis test result with an image scale 1/6000 are also introduced by Grejner-Brzezinska (1999) and Toth (1999).

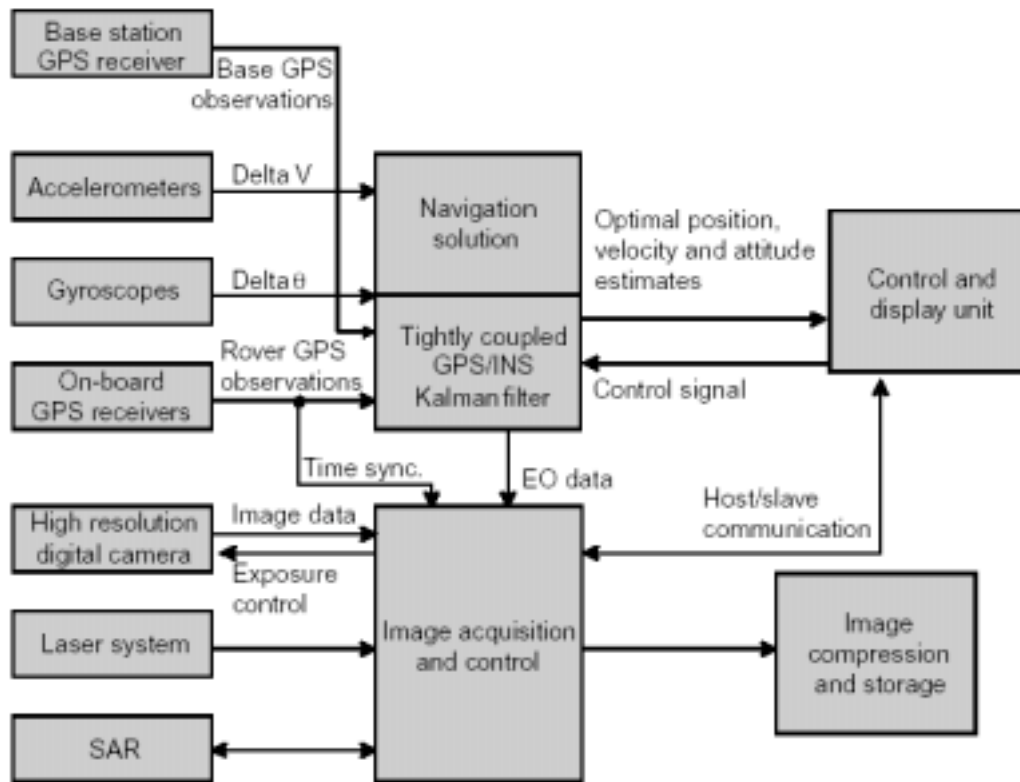


Figure 6.1: The conceptual structure of AIMS (Grejner-Brzezinska and Toth, 1998).

Table 6.1: System parameters of AIMS (Grejner-Brzezinska and Toth, 1998)

<i>Kalman Filter States</i>	<i>Number of states</i>
Navigation parameters	
- Position errors	3
- Velocity errors	3
- Attitude errors	2
- Heading errors	1
Accelerometer errors (random walk)	
- Biases	3
- Scale factor errors	3
Gyro errors (random walk)	
- Drifts	3
Gravity	

- Deflection (Gauss-Markov, 20 nmi)	2
- Anomaly (Gauss-Markov, 20 nmi)	1
GPS errors	
- Ionospheric delay (random walk)	Number of double differences

The Applanix Corporation in Canada has developed an off-the-shelf Position and Orientation System for Direct Georeferencing (POS/DG) for airborne applications and several test projects in collaboration with University of Calgary are implemented (Lithopoulos, 1999; Mostafa and Schwarz, 2000). Scherzinger (2000) described two levels of inertial-GPS integration for the purpose of obtaining inertially aided real-time kinematic. A loosely coupled integration has the advantage of being generic and simple to implement, and the disadvantages of no visibility of user into the functions beyond the interface specification and dropping down the loosing navigation solution when fewer than 4 GPS satellites are visible. In a tightly coupled integration, the GPS receiver is used as a source of observables and satellite orbital and clock parameters. The integer ambiguity search function is combined with the integration Kalman filter, so that i) there is no limit on visibility of data/information between these modules, and ii) the integer ambiguity search is by construction inertially aided. Furthermore the benefit of tightly coupled inertial-GPS integration, i.e. uses observables data when fewer than 4 satellites are visible, is realized.

The POS/DG system is tested with several image sensors. Different calibration methods of the integrated system such as, airborne calibration and terrestrial calibration, are explained and performance analysis of the system with low-cost digital cameras is reported by Mostafa and Schwarz (2001), Mostafa and Hutton (2001), and Mostafa (2002).

In the University of Stuttgart, the sensor integration and system calibration issues for three line scanner imagery are discussed by Cramer, Stallmann, and Haala (1999). For the test flights, a strapdown INS is used and the GPS/INS data are combined in the aerial triangulation. System calibration issues including self-calibration are provided by Cramer and Stallmann (2002). In addition, Terzibaschian and Scheele (1994) introduced the attitude and positioning system used for georeferencing of WAOSS three-line scanner. Poli (2001) provided a sensor model for direct georeferencing of three-line scanner (TLS) images using GPS/INS observations for external orientation. However, no Kalman filtering method is implemented in these studies.

A new combined block adjustment approach using GPS data is introduced from the University of Hannover. GPS ambiguity terms are improved using the independent position information from the bundle adjustment (Jakobsen, 1996). After this, GPS and IMU data are together combined in a bundle solution (Jakobsen 1999). The potential and limitation of this combined sensor orientation is

evaluated by Jakobsen (2000). The calibration aspects of the sensors are provided by Jakobsen (2002) and Wegmann (2002).

Another integrated system calibration and combined block adjustment work related with the OEEPE test is reported by Forlani and Pinto (2002).

Azizi et al. (2001) provide a solution with GPS/INS data and GCPs with a Kalman filtering approach during the phototriangulation. Requirements for the Kalman filtering process are satisfied by employing standard collinearity condition equations as the prediction model. The state vector in this problem is considered to include the coordinates of the projection centers of the camera during the exposure time, camera orientation parameters, and the ground coordinates of the tie points. measurement model linear interpolation algorithm that accepts the GPS/INS observables during the aerial photography flight mission. Any additional observations such as the coordinates of the ground control points may also be tailored into the measurement model.

## 7 CONCLUSIONS AND FUTURE WORK

The usage of GPS and INS for the solutions of navigation problems in photogrammetric applications provide a challenging opportunity in the last decade. Basically, there are two different approach for georeferencing of airborne imagery using GPS and INS data. Direct georeferencing gives the exterior orientation parameters, projection center coordinates and attitude data, as the result of navigation process with GPS and INS observations without using control points in the navigation solution for airborne imagery. The precision of the georeferencing depends on the application parameters such as, image scale, camera specifications, etc. However, the accuracy results of directgeoreferencing reported in the literature is still 2-3 time lower than the traditional photogrammetric aerotriangulation results (Heipke et al., 2002).

The second approach for georeferencing includes an integrated solution of GPS/INS data together with ground control and tie points in the bundle block adjustment process. This process provides the same accuracy with traditional triangulation methods. In addition, out of the topic of this report, only GPS measurements can be added to the photogrammetric triangulation (Gruen et al, 1993; Ackermann, 1996; ASPRS, 1996). However, an integration with INS reduces the errors of GPS position data and provides attitude data.

There are GPS/INS integration solutions without any noise filtering. However, application of a linear filtering methods provides better positioning and attitude estimation results. In GPS/INS case, Dicrete Kalman Filtering is commonly performed to the integration projects in the literature. Since the designed GPS/INS systems varies almost in every project, different Kalman filters are implemented for each. Centralized and decentralized filter approaches are applied to the integrated systems designed in loosely coupled or tightly coupled manner. Both filtering approaches have their own advantages and disadvantages. In general, decentralized approach is preferred due to the flexibility in INS selection. Centralized approach is preferred for tightly coupled devices.

Since the INS systems cost much more than GPS, the research trends go towards low-cost IMUs. Due to the strapdown INS systems are cheaper than the platform systems, for airborne georeferencing projects, strapdown INSs are integrated with GPS. The Kalman filtering designs are also developed for this kind of integrations. No platform (gimbaled) INS/GPS integration report could be found in the literature. However, gimbaled systems provide higher accuracy. A future work can be done using this type of INS systems.

Another distinction can be done according to the image sensor type used. SAR, laser scanners, analog frame cameras, frame CCD cameras, and pushbroom line cameras can be said as the basic

sensor types for aerial applications. The most common georeferencing applications are done using analog or CCD frame cameras. The system implementation using Kalman filter approach are also reported for this type of sensors. Although some authors mentioned in section six were worked on pushbroom CCD systems, no filtering approach for GPS/INS observations can be found. New investigations can be done with directgeoreferencing of line CCD cameras with GPS/INS.

## REFERENCES

- [1] **Ackermann F.**, “*Experimental Tests on Fast Ambiguity Solutions for Airborne Kinematic GPS Positioning*”, ISPRS International Symposium, Vol. XXXI, Part B6, p. 51-56, Vienna, Austria, July 1996.
- [2] **American Society for Photogrammetry and Remote Sensing (ASPRS)**, “*Digital Photogrammetry: An Addendum to the Manual of Photogrammetry*”, ASPRS Publications, 1996.
- [3] **Azizi A., Sharifi M.A., Parian J.A.**, “*A New Approach for the Mathematical Modeling of the GPS/INS Supported Phototriangulation Using Kalman Filtering Process*”, KIS 2001 International Symposium On Kinematic Systems In Geodesy, Geomatics And Navigation, The Banff Centre Banff, Canada, June 5 - 8, 2001.
- [4] **Colomina I.**, “*Modern Sensor Orientation Technologies and Procedures*”, OEEPE Integrated Sensor Orientation Test Report and Workshop Proceedings, Official Publication No. 43, July 2002.
- [5] **Cramer M.**, “*GPS/INS Integration*” in Fritsch/Hobbie (eds), Photogrammetric Week 1997, Stuttgart, Germany, pp. 1-10, 1997.
- [6] **Cramer M.**, “*Direct Geocoding – is Aerial Triangulation Obsolete?*” in Fritsch/Spiller (eds), Photogrammetric Week 1999, Wichmann Verlag, Heidelberg, Germany, pp. 59-70, 1999.
- [7] **Cramer M., Haala N.**, “*Direct exterior orientation of airborne sensors - an accuracy investigation of an integrated GPS/inertial system*”, in 'Proc. ISPRS Workshop Comm. III/1', Portland, Maine, USA, 1999.
- [8] **Cramer M., Stallmann D., Haala N.**, “*Sensor integration and calibration of digital airborne three-line camera systems*”, in 'Proc. ISPRS Workshop Comm. II/1', Bangkok, Thailand, 1999.
- [9] **Cramer M., Stallmann D., Haala N.**, “*Direct Georeferencing Using GPS/Inertial Exterior Orientations for Photogrammetric Applications*”, IAPRS Vol. XXXIII, Amsterdam, 2000.
- [10] **Cramer M.**, “*On the use of Direct Georeferencing in Airborne Photogrammetry*”, 3<sup>rd</sup> International Symposium on Mobile Mapping Technology, Digital Publication on CD, Cairo, Egypt, January 2001.
- [11] **Cramer M., Stallmann D.**, “*System Calibration for Direct Georeferencing*”, ISPRS Comm. III Symposium ‘Photogrammetric Computer Vision’, Graz, Austria, 9-13 September 2002.
- [12] **Dowman I.**, “*Orientation of SAR Data: Requirements and Applications*”, Integrated Sensor Orientation, Colomina/ Navarro (eds.), Wichmann Verlag, Heidelberg, Germany, 1995.

- [13] **El-Sheimy N.**, “*Report on Kinematic and Integrated Positioning Systems*” FIG XXII International Congress, Washington, D.C. USA, April 19-26 2002.
- [14] **Favey E., Cerniar M., Cocard M., Geiger A.**, “*Sensor Attitude Determination Using GPS Antenna Array and INS*”, ISPRS WG III/1 Workshop: ‘Direct versus Indirect Methods of Sensor Orientation’, Barcelona, 25-26 November 1999.
- [15] **Forlani G., Pinto L.**, “*Integrated INS/DGPS Systems: Calibration and Combined Block Adjustment*”, OEEPE Integrated Sensor Orientation Test Report and Workshop Proceedings, Official Publication No. 43, pp. 11-18, July 2002.
- [16] **Gelb A.**, “*Applied Optimal Estimation*”, The M.I.T. Press, Massachusetts Institute of Technology, Massachusetts, U.S.A., 1974.
- [17] **Grejner-Brzezinska D. A., Toth C. K.**, “*GPS Error Modeling and OTF Ambiguity Resolution for High-Accuracy GPS/INS Integrated System*”, Journal of Geodesy, vol. 72, pp. 626-638, 1998.
- [18] **Grejner-Brzezinska D. A., Wang J.**, “*Gravity Modeling for High-Accuracy GPS/INS Integration*”, Navigation, Vol. 45, No 3, pp. 209-220, 1998.
- [19] **Grejner-Brzezinska D. A.**, “*Direct Exterior Orientation of Airborne Imagery with GPS/INS System: Performance Analysis*”, Navigation, Vol. 46, No. 4, pp. 261-270, 1999.
- [20] **Grejner-Brzezinska D. and Toth C.** “*Precision Mapping of Highway Linear Features*”, Geoinformation for All, Proceedings, XIXth ISPRS Congress, Amsterdam, Netherlands, pp. 233-240, 16-23 July 2000.
- [21] **Grewal M. S., Weill L. R., Andrews A. P.**, “*Global Positioning Systems, Inertial Navigation, and Integration*”, John Wiley and Sons Publication, New York, U.S.A., 2001.
- [22] **Gruen A.**, “*Algorithmic Aspects in On-line Triangulation*”, IAPRS Vol. 25-A3, Rio de Janeiro, Brasil, pp. 342-362, 1984.
- [23] **Gruen A., Cocard M., Kahle H.G.**, “*Photogrammetry and Kinematic GPS: Results of a High Accuracy Test*”, PE&RS Vol. 59, No 11, pp. 1643-1650, November 1993.
- [24] **Heipke et al.**, “*Test Goals and Test Set Up for the OEEPE Test: Integrated Sensor Orientation*”, OEEPE Integrated Sensor Orientation Test Report and Workshop Proceedings, Official Publication No. 43, pp. 11-18, July 2002.
- [25] **Jakobsen K., Schmitz M.**, IAPRS Vol. XXXI, Part B3, pp. 355-359, Vienna, 1996.
- [26] **Jakobsen K.**, “*Determination of Image Orientation Supported by IMU and GPS*”, Joint Workshop of ISPRS Working Groups I/1, I/3 and IV/4 – Sensors and Mapping from Space, Hannover, 1999.

- [27] **Jakobsen K.**, “*Potential and Limitation of Direct Sensor Orientation*”, IAPRS vol. XXXIII, Part B3, pp. 429-435, Amsterdam, 2000.
- [28] **Jakobsen K.**, “*Calibration Aspects in Direct Georeferencing of Frame Imagery*”, ISPRS Com. I, Midterm Symposium, Integrated Remote Sensing at the Global, Regional, and Local Scale, Denver, U.S.A., 10-15 November 2002.
- [29] **Kalman R. E.**, “*A New Approach to Linear Filtering and Prediction Problems*”, Transactions of the ASME-Journal of Basic Engineering, No. 82, Series D, pp. 35-45, 1960.
- [30] **Klingelé E.E., Bagnaschi L., Halliday M., Cocard M., Kahle H.G.**, “*Airborne Gravimetric Survey of Switzerland*”, Technical Report No. 239, ETH Swiss Federal Institute of Technology, Institute of Geodesy and Photogrammetry, Switzerland, June 1994.
- [31] **Lithopoulos E.**, “*The Applanix Approach to GPS/INS Integration*” in Fritsch/Spiller (eds), Photogrammetric Week 1999, Wichmann Verlag, Heidelberg, Germany, pp. 53-57, 1999.
- [32] **Lutes J.**, “*DAIS: A Digital Airborne Imaging System*”, Pecora 15/Land Satellite Information IV/ISPRS Commission I Midterm Symposium/FIEOS Conference Proceedings, Denver, CO U.S.A., 10-15 Nov 2002.
- [33] **Mostafa M.M.R., Schwarz K.P.**, “*A Multi-Sensor System for Airborne Image Capture and Georeferencing*”, PE&RS, Vol. 66, No. 12, pp. 1417-1423, December 2000.
- [34] **Mostafa M.M.R., Schwarz K.P.**, “*Digital Image Georeferencing from a Multiple Camera System by GPS/INS*”, ISPRS Journal of Photogrammetry and Remote Sensing, Vol. 56, pp. 1-12, 2001.
- [35] **Mostafa M.M.R., Hutton J.**, “*Airborne Kinematic Positioning and Attitude Determination Without Base Stations*”, International Symposium on Kinematic Systems in Geodesy, Geomatics, Navigation (KIS 2001), Banff, Alberta, Canada, 4-8 June 2001.
- [36] **Mostafa M.M.R.**, “*Digital Multi-Sensor Systems – Calibration and Performance Analysis*”, Integrated Sensor Orientation, Test Report and Workshop Proceedings, OEEPE Official Publication No. 43, July 2002.
- [37] **Madani M., Wang Y., Mostafa M.**, “*Direct EO QC/QA Tools in Automatic Aerial Triangulation*”, White Paper, Z/I Imaging, <http://www.ziimaging.com/News/default.htm>, Last accessed: 14.01.2003.
- [38] **Salzmann M. A.**, “*Least Squares Filtering and Testing for Geodetic Navigation Applications*”, Ph.D. Thesis, Delft University of Technology, Dept. of Geodetic Engineering, Delft, Holland, 1993.

- [39] **Sanchez R. D., Hothem L. D.**, “*Positional Accuracy of Airborne Integrated Global Positioning and Inertial Navigation Systems for Mapping in Glen Canyon, Arizona*”, Open-File Report 02-222, U.S. Geological Survey, U.S.A, 2001.
- [40] **Scherzinger B. M.**, “*Precise Robust Positioning with Inertial/GPS RTK*”, ION GPS 2000, 13<sup>th</sup> International Technical Meeting of the Satellite Division of the Institute of Navigation, Salt Lake City, Utah, U.S.A., 19-22 September 2000.
- [41] **Schwarz K.P., Chapman M.A., Cannon M.E., Gong P., Cosandier D.**, “*A Precise Positioning/Attitude System in Support of Airborne Remote Sensing*”, Canadian Conference on GIS-94/ ISPRS, pp. 191-201, 6-10 June 1994.
- [42] **Schwarz, K.P.** “*Integrated Airborne Navigation Systems for Photogrammetry*”, Proc. Photogrammetric Weeks ‘95, Stuttgart, pp. 139-153, September 11-14, 1995.
- [43] **Skaloud J.**, “*Optimizing Georeferencing of Airborne Survey Systems by INS/DGPS*”, Ph.D. Thesis, The Uni. of Calgary, Dept. of Geomatics Engineering, Calgary, Alberta, 1999.
- [44] **Skaloud J., Bruton A.M., Schwarz K.P.**, “*Detection and Filtering of Short-Term ( $1/f^{\alpha}$ ) Noise in Inertial Sensors*”, Navigation: Journal of the Institute of Navigation, vol. 46, No 2, pp. 97-107, Summer 1999.
- [45] **Skaloud J.**, “*Problems in Direct-Georeferencing by INS/DGPS in the Airborne Environment*”, Invited Paper, ISPRS Workshop on ‘Direct versus Indirect Methods of Orientation’ WG III/1, Barcelona, 25-26 November 1999.
- [46] **Skaloud J., Schwarz K.P.**, “*Accurate Orientation for Airborne Mapping Systems*”, PE&RS, Vol. 66, No. 4, pp. 393-401, April 2000.
- [47] **Terzibaschian T., Scheele M.**, “*Attitude and Positioning Measurements Systems used in the Airborne Testing of the Original Mars Mission Wide Angle Optoelectronic Stereo Scanner WAOSS*”, IAPRS Vol. 30, Part I, pp. 47-55, 1994.
- [48] **Toth C., Grejner-Brzezinska, D. A.**, “*Performance Analysis of the Airborne Integrated Mapping System (AIMS™)*”, ISPRS Commission II Symposium on Data Integration: Systems and Techniques, July 13-17, Cambridge, England, pp.320-326, 1998.
- [49] **Toth C.**, “*Experiences with frame CCD Arrays and Direct Georeferencing*” in Fritsch/Spiller (eds), Photogrammetric Week 1999, Wichmann Verlag, Heidelberg, Germany, pp. 95-109, 1999.
- [50] **Wang J., Lee H.K., Rizos C.**, “*GPS/INS Integration: A Performance and Sensitivity Analysis*”, 4<sup>th</sup> Symposium on GPS/GNSS, Wuhan, China, 6-8 November 2002.

- [51] **Wegmann H.**, “*Image Orientation by Combined (A)AT with GPS and IMU*”, ISPRS Com. I, Midterm Symposium, Integrated Remote Sensing at the Global, Regional, and Local Scale, Denver, U.S.A., 10-15 November 2002.
- [52] **Welch G., Bishop, G.**, “*An Introduction to the Kalman Filter*”, Technical Report 95-041, University of North Carolina, Dept. of Computer Science, March 2002.

## APPENDIX

### RANDOM PROCESSES: BASIC CONCEPTS

A *random variable* is a function whose values depend on the outcome of a chance event. The *values* of a random variable may be any convenient mathematical entities; real or complex numbers, vectors, etc. For simplicity, we shall consider here only real-valued random variables, but this is no real restriction. Random variables will be denoted by  $x, y, \dots$  and their values by  $\xi, \eta, \dots$ . Sums, products, and functions of random variables are also random variables.

A random variable  $x$  can be explicitly defined by stating the probability that  $x$  is less than or equal to some real constant  $\xi$ . This is expressed symbolically by writing

$$Pr(x \leq \xi) = F_x(\xi); F_x(-\infty) = 0, F_x(+\infty) = 1$$

$F_x(\xi)$  is called the *probability distribution function* of the random variable  $x$ . When  $F_x(\xi)$  is differentiable with respect to  $\xi$ , then  $f_x(\xi) = dF_x(\xi)/d\xi$  is called the *probability density function* of  $x$ .

The *expected value* (*mathematical expectation*, *statistical average*, *ensemble average*, *mean*, etc., are commonly used synonyms) of any nonrandom function  $g(x)$  of a random variable  $x$  is defined by

$$Eg(x) = E[g(x)] = \int_{-\infty}^{\infty} g(\xi) dF_x(\xi) = \int_{-\infty}^{\infty} g(\xi) f_x(\xi) d\xi \quad (1)$$

As indicated, it is often convenient to omit the brackets after the symbol  $E$ . A sequence of random variables (finite or infinite)

$$\{x(t)\} = \dots, x(-1), x(0), x(1), \dots \quad (2)$$

is called a *discrete* (or *discrete-parameter*) *random* (or *stochastic*) *process*. One particular set of observed values of the random process (2)

$$\dots, \xi(-1), \xi(0), \xi(1), \dots$$

is called a *realization* (or a *sample function*) of the process. Intuitively, a random process is simply a set of random variables, which are indexed in such a way as to bring the notion of time into the picture.

A random process is *uncorrelated* if

$$Ex(t)x(s) = Ex(t)Ex(s) \quad (t \neq s)$$

If, furthermore,

$$Ex(t)x(s) = 0 \quad (t \neq s)$$

then the random process is *orthogonal*. Any uncorrelated random process can be changed into orthogonal random process by replacing  $x(t)$  by  $x'(t) = x(t) - Ex(t)$  since then,

$$Ex'(t)x'(s) = E[x(t) - Ex(t)][x(s) - Ex(s)] = Ex(t)x(s) - Ex(t)Ex(s) = 0$$

If a random process is orthogonal, then,

$$E[x(t_1) + x(t_2) + \dots]^2 = Ex^2(t_1) + Ex^2(t_2) + \dots \quad (t_1 \neq t_2 \neq \dots)$$

If  $\mathbf{x}$  is a vector-valued random variable with components  $x_1, \dots, x_n$  (which are of course random variables), the matrix

$$[E(x_i - Ex_i)(x_j - Ex_j)] = E(\mathbf{x} - E\mathbf{x})(\mathbf{x}' - E\mathbf{x}') = \text{cov } \mathbf{x} \quad (3)$$

is called the *covariance matrix of x*.

A random process may be specified explicitly by stating the probability of simultaneous occurrence of any finite number of events of the type

$$x(t_1) \leq \xi_1, \dots, x(t_n) \leq \xi_n; \quad (t_1 \neq \dots \neq t_n), \text{ i.e., } Pr[(x(t_1) \leq \xi_1, \dots, x(t_n) \leq \xi_n)] = F_{x(t_1), \dots, x(t_n)}(\xi_1, \dots, \xi_n) \quad (4)$$

where  $F_{x(t_1), \dots, x(t_n)}$  is called the *joint probability distribution function* of the random variables  $(x(t_1), \dots, x(t_n))$ . The *joint probability density function* is then

$$f_{x(t_1), \dots, x(t_n)}(\xi_1, \dots, \xi_n) = \partial^n F_{x(t_1), \dots, x(t_n)} / \partial \xi_1 \dots \partial \xi_n$$

provided the required derivatives exist. The expected value  $Eg[x(t_1), \dots, x(t_n)]$  of any nonrandom function of  $n$  random variables is defined by an  $n$ -fold integral analogous to (1).

A random process is *independent* if for any finite  $t_1 \neq \dots \neq t_n$ , (4) is equal to the product of the first-order distributions

$$Pr[x(t_1) \leq \xi_1] \dots Pr[x(t_n) \leq \xi_n]$$

If a set of random variables is independent, then they are obviously also uncorrelated. The converse is not true in general. For a set of more than 2 random variables to be independent, it is not sufficient that any pair of random variables be independent.

Frequently it is of interest to consider the probability distribution of a random variable  $x(t_{n+1})$  of a random process given the actual values  $\xi(t_1), \dots, \xi(t_n)$  with which the random variables  $x(t_1), \dots, x(t_n)$  have occurred. This is denoted by

$$Pr[x(t_{n+1}) \leq \xi_{n+1} | x(t_1) = \xi_1, \dots, x(t_n) = \xi_n] = \frac{\int_{-\infty}^{\xi_{n+1}} f_{x(t_1), \dots, x(t_{n+1})}(\xi_1, \dots, \xi_{n+1}) d\xi_{n+1}}{f_{x(t_1), \dots, x(t_n)}(\xi_1, \dots, \xi_n)} \quad (5)$$

which is called the *conditional probability distribution function* of  $x(t_{n+1})$  given  $x(t_1), \dots, x(t_n)$ . The *conditional expectation*

$$E\{g[x(t_{n+1})]|x(t_1), \dots, x(t_n)\}$$

is defined analogously to (1). The conditional expectation is a random variable; it follows that

$$E[E\{g[x(t_{n+1})]|x(t_1), \dots, x(t_n)\}] = E\{g[x(t_{n+1})]\}$$

In all cases of interest in this paper, integrals of the type (1) or (5) need never be evaluated explicitly, only the *concept* of the expected value is needed.

A random variable  $x$  is *gaussian* (or *normally distributed*) if

$$f_x(\xi) = \frac{1}{[2\pi E(x - Ex)^2]^{1/2}} \exp \left[ -\frac{1}{2} \frac{(\xi - Ex)^2}{E(x - Ex)^2} \right]$$

which is the well-known bell-shaped curve. Similarly, a random vector  $\mathbf{x}$  is *gaussian* if

$$f_x(\xi) = \frac{1}{(2\pi)^{n/2} (\det \mathbf{C})^{1/2}} \exp \left[ -\frac{1}{2} (\xi - E\mathbf{x})' \mathbf{C}^{-1} (\xi - E\mathbf{x}) \right]$$

where  $\mathbf{C}^{-1}$  is the inverse of the covariance matrix (3) of  $\mathbf{x}$ . A *gaussian random process* is defined similarly.

The importance of gaussian random variables and processes is largely due to the following facts:

**Theorem:** (A) *Linear functions (and therefore conditional expectations) on a gaussian random process are gaussian random variables.*

(B) *Orthogonal gaussian random variables are independent.*

(C) *Given any random process with means  $Ex(t)$  and covariances  $Ex(t)x(s)$ , there exists a unique gaussian random process with the same means and covariances. (Kalman, 1960)*